LA-UR-12-26638
Approved for public release; distribution is unlimited.

Title:	Characterization of the Mechanical Properties of DAP and Seabreeze
Author(s):	Cady, Carl M. Liu, Cheng Lovato, Manuel L.
Intended for:	Report

Characterization of the Mechanical Properties of DAP and Seabreeze

Carl Cady, Cheng Liu and Manuel Lovato, MST-8

I. Introduction

The primary reason for this investigation was to determine the most accurate means of measuring the effect of aging in these materials. Initial characterization was pursued to find the most sensitive, repeatable test that would have the least amount of scatter in the test results. Preliminary investigations let to the conclusion that the fracture toughness would likely be the property to show the greatest change in behavior for any intrinsic material property. Test configurations that were initially considered were tensile tests, 3 and 4 point bend tests, Brazil tests, Brazil tests with initial damage and finally a test geometry that is being called a "compression – fracture" test. The tensile test will continue to be done because it will be used to generate information about the Poisson's ratio, which can be used in simulations that would verify the test results presented in this report. The bend bar and Brazil test configurations were tried and determined to be unsuitable because they allowed for unstable crack growth in the materials. The result of these investigations on un-pedigreed materials leading to the selection and use of a test geometry that has subsequently been used on pedigreed materials is the focus of this report.

II. Materials

The materials characterized in this report were from varying sources but were made the same way with the same constituents. Initial work was carried out on un-pedigreed "poker chip" samples that were made for a different project. These samples were used because that were nominally the same as the materials of interest and because they were readily available at the beginning of this work. All sample geometry evaluation was conducted on these un-pedigreed materials. Once the final "compression-fracture" sample was chosen further evaluation was conducted on pedigreed materials. Additionally, samples were artificially aged from both pedigreed and un-pedigreed materials to be able to compare the results to similar processes.

III. Experimental methods

All mechanical testing was conducted on an Instron 1125 electro-mechanical load frame with a MTS "renew" control package. A sub press was used to ensure axial loading and minimize the risk of off axis deflection. No lubrication was used at the loading surfaces between the frame and the sample. The samples were expected to behave in a brittle manner and have little strain to failure, therefore, lubrication was though to be unnecessary.

The characterization technique used to measure displacement and strain in these experiments is the digital image correlation (DIC). DIC has been demonstrated to be robust, flexible, applicable to large deformation and over a wide range of size scales and very affordable (as sophisticated optics instrumentation is usually not required). The underlying principle of digital image correlation as a deformation measurement technique is rather simple. It relies on the computer vision approach to extract the whole-field displacement data, that is, by comparing the features in a pair of digital images of a specimen surface before and after deformation. Since the displacements are calculated directly by correlating the two digital images, processing of fringe

patterns or other secondary phenomena to yield deformations is not required.

The basis of two-dimensional digital image correlation (2D-DIC) for the measurement of surface displacements is the matching of one point from the image of an object's surface before loading (image of the undeformed object) to a point in the image of the object's surface taken at a later time/loading (image of the deformed object). Assuming a one-to-one correspondence between the deformations in the image recorded by the CCD camera and the deformations of the surface of the object, an accurate, point-to-point mapping from the undeformed image to the deformed image will allow the displacement of the object's surface to be measured. Two main requirements must be met for the successful use of 2D-DIC. First, in order to provide features for the matching process, the surface of the object must have a pattern that produces varying intensities of diffusely reflected light from its surface. This pattern may be applied to the object or it may occur naturally. Secondly, the imaging camera must be positioned so that its sensor plane is parallel to the surface of the planar object.

Consider a planar object illuminated by a light source and suppose that the object undergoes two-dimensional planar deformation. Let $\mathbb{R}$ be a small region of the undeformed object and $\mathbb{R}_*$ be the same region but in the deformed configuration. The light intensity pattern of the undeformed region $\mathbb{R}$ is denoted by $I(\boldsymbol{x})$, where $\boldsymbol{x} \in \mathbb{R}$, while the light intensity pattern of the deformed region $\mathbb{R}_*$ is denoted as $I_*(\boldsymbol{y})$, where $\boldsymbol{y} \in \mathbb{R}_*$ and $\boldsymbol{y} = \hat{\boldsymbol{y}}(\boldsymbol{x})$ specifies the mapping relation, which connects the material particle that is located at $\boldsymbol{x}$ prior to the deformation and its current position $\boldsymbol{y}$. Both $I(\boldsymbol{x})$ and $I_*(\boldsymbol{y})$ are assumed to be in unique and one-on-one correspondence with the respective object surface, and they are integer-valued functions ranging from 0 to 255 when using an 8-bit gray-scale digital camera. If during the deformation process, the intensity pattern only deforms but does not alter its local value, then we should have

$$I_*(\boldsymbol{y}) = I_*\big(\hat{\boldsymbol{y}}(\boldsymbol{x})\big) = I(\boldsymbol{x}), \qquad \forall\, \boldsymbol{x} \in \mathbb{R}.$$

As a result, the measurement of the displacement field using DIC can be formulated into the following mathematical problem: By knowing the two intensity patterns $I(\boldsymbol{x})$ and $I_*(\boldsymbol{y})$ of the same region before and after deformation, find a mapping relation $\boldsymbol{y} = \hat{\boldsymbol{y}}(\boldsymbol{x})$, such that

$$I_*\big(\hat{\boldsymbol{y}}(\boldsymbol{x})\big) - I(\boldsymbol{x}) = 0, \qquad \forall\, x \in \mathbb{R}.$$

Furthermore, if the deformation is homogeneous within the small region $\mathbb{R}$, i.e., if the deformation is such that

$$\hat{\boldsymbol{y}}(\boldsymbol{x}) = \boldsymbol{F}\,\boldsymbol{x} + \boldsymbol{b},$$

where $\boldsymbol{F}$ is a constant tensor and $\boldsymbol{b}$ a constant vector. For two-dimensional deformation, the above mathematical problem becomes to find a matrix $\boldsymbol{F}$ with four unknown scalar components, and a vector $\boldsymbol{b}$ with two unknown scalar components, such that

$$I_*(\boldsymbol{F}\,\boldsymbol{x} + \boldsymbol{b}) - I(\boldsymbol{x}) = 0, \qquad \forall\, \boldsymbol{x} \in \mathbb{R},$$

with the restriction of $\det\{\boldsymbol{F}\} > 0$. The displacement field $\boldsymbol{u}$ is related to $\boldsymbol{F}$ and $\boldsymbol{b}$ through $\boldsymbol{u}(\boldsymbol{x}) = (\boldsymbol{F} - \boldsymbol{I})\,\boldsymbol{x} + \boldsymbol{b}$, where $\boldsymbol{I}$ is the identity tensor.

In order to obtain the numerical values of components of $\boldsymbol{F}$ and $\boldsymbol{b}$, we need to compare two intensity patterns of the object before and after deformation. Therefore, the basic problem for the surface displacement measurement is to correlate the two images. This is usually achieved by minimizing (or maximizing) some correlation coefficients. One such correlation coefficient is the so-called least-square coefficient defined by

$$C(\boldsymbol{F}, \boldsymbol{b}) = \frac{\sum_{x\in\mathbb{R}}\{I_*(\boldsymbol{F}\,\boldsymbol{x} + \boldsymbol{b}) - I(\boldsymbol{x})\}^2}{\sum_{x\in\mathbb{R}} I^2(\boldsymbol{x})}.$$

Note that $C(\boldsymbol{F}, \boldsymbol{b}) = 0$ corresponds to perfect correlation and to find the components of $\boldsymbol{F}$ and $\boldsymbol{b}$,

one needs to minimize the function $C(\boldsymbol{F}, \boldsymbol{b})$ given in the above equation. More detailed descriptions of the DIC technique can be found in literature, e.g., Sutton et al. [1].

The advantage to using DIC is that the images can be used to look at both the global strain and local strain, and it is possible to reanalyze the data in many different ways. This means that it is possible to get a large amount of information from a single experiment. The DIC technique can detect motion as small as 0.02 pixels. As a result, if the gage section is 100 pixels across in the image, the accuracy of strain measurement will be 0.02%, assuming the deformation in the gage section is uniform. The larger the image size the higher accuracy of measurement can achieve.

In this analysis we have two data files that are created simultaneously. 1) From the camera system we get time – strain (engineering). This data is calibrated from the dimensions of the sample and also uses a relative displacement of markers placed on the specimen before loading. 2) The other system is the calibrated load frame. From this system time, displacement and load are stored. The load – time file is generated to go with the images that were captured from the image system for the DIC analysis. This step is done to synchronize the time-load with the time-strain information from the DIC file. Since the strain from the DIC technique does not have any machine compliance, it very accurately shows the early loading stages. It is essentially like putting a strain gage of variable size or multiple strain gages on the test specimen. Further details on the stress analysis for the various geometries will be described in the section on sample geometry.

The digital images taken during a test at discreet time intervals are analyzed to measure fine differences between sequential images. These differences become the basis for determining the strains in the sample. It also enables us to determine when crack initiate because crack initiation is also the same at the sample location and time when the "image correlation" begins to break down. It is through this correlation breakdown that we can measure both the crack length and the crack growth rates. Both measurements are useful and necessary in in order to calculate fracture toughness.

IV. Sample Geometries

Initially the test configuration for this experimental work was to ne conducted using 3- or 4-point bend samples. For DAP the sample geometry was to be 2.25" x 0.375" by 0.189" and for the seabreeze material the geometry was specified as 3"x 0375"x 0375" the test span to be set at 2 inches. Since little work had been done on these materials before basic material understanding was necessary and "un-pedigreed" materials were found and used to develop a test plan. The source of the unpedigreed materials came from "poker chips" or disks that were 1.25" diameter 0.125" thick with a center hole of ~ 0.145". The seabreeze disks had a starting geometry of 1.13" diameter and 0.125" thick, again with a 0.145" center hole. Initial tensile samples were machined from these chips that had a gage dimension of 0.55" length x 0.125" width and 0.125" thickness. It was possible to measure the Poisson's ratio of these tensile samples using the DIC technique described above. In addition to the tensile samples small Brazil disk samples were made from the original "chips". These small, uniform Brazil specimens had a diameter of 0.5" and a thickness of 0.125" thick. The original "chips" were also tested as is as an additional type of modified Brazil test. The Brazil tests were conducted based on the work of Huang, *et. al*.[2]and Liu, et. al.[3] Based on the testing of these samples it was decided to further modify the poker chip samples to see if the geometry of the sample could be used to slow down the crack growth rate in

the sample. The sample geometry was chosen based on work of Sammis and Ashby [4] and Nemat-Nasser, *et.al*.[5]. In this case a rectangular sample with a center hole was used as the new test sample. It will be referred to as the "compression- fracture" (CF) sample throughout this report. The DAP CF sample was 1.14" in length, 0.5" width and 0.125" thick with the 1/8" hole centered on length and width. The only difference for the seabreeze sample and the DAP was length. It was only 0.95" in length.

Based on the test results of the Brazil, mini-Brazil and compression fracture the test geometry for the pedigreed samples was re-evaluated. It was decided that three CF samples would be generated from each of the seabreeze bars and two CF samples would come from the DAP bend bars. The dimensions of the pedigreed seabreeze samples was 0.95" length x 0.375" width x 0.375" thick with the hole centered on the length and width. The DAP samples had dimensions of 1.12" length x 0.375" width x 0.189" thick with a centered hole.

V. Experimental results

V.1 Tensile Results

Initial tests results of the tensile tests for the DAP components are presented in Figures 1and 2. The first set of plots shows the stress strain behavior of the materials (Fig.1). The slope of the stress strain curves gives the modulus of the material. For Dap the modulus was measured to be 4.97 ± 0.28 GPa. The second pair of plots shows the lateral strain versus axial strain (Fig.2). From this plot it is possible to calculate the poisons ratio for these materials by measuring the slope of the lines. Poisson's ratio was measured for DAP to be 0.38 ± 0.04. Typical strain field maps for the tensile tests are shown in figure 3. These maps were generated for a DAP sample. It is important to note that the overall strain is quite small and there is very little curvature in the stress strain curve typical of brittle materials.

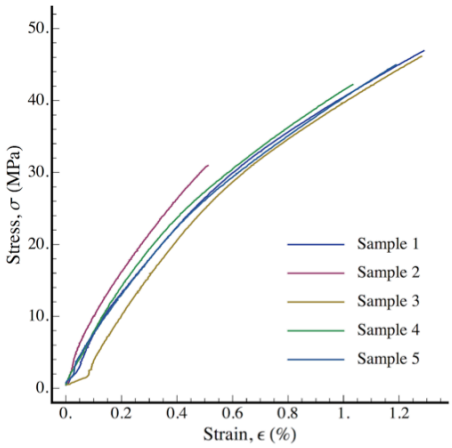

Figure 1. Tensile Stress strain plots for DAP.

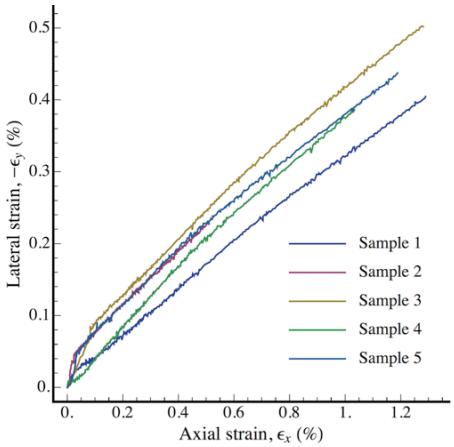

Figure 2. Lateral strain versus axial strain plot used to measure Poisson's ratio for DAP the material.

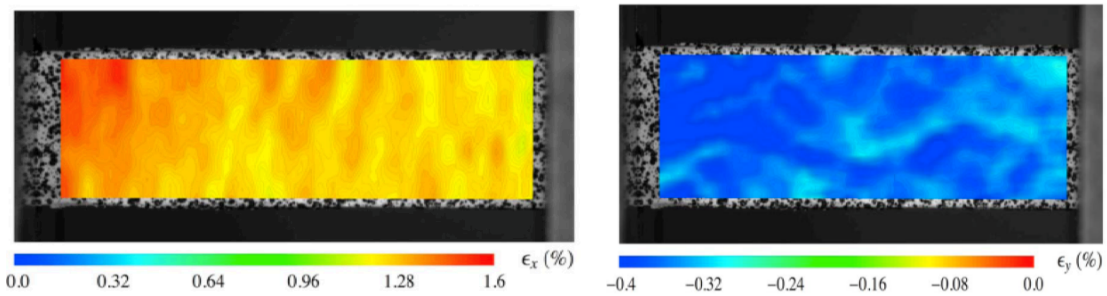

a) b)

Figure 3. Digital image correlation strain maps for a typical tensile testfor the DAP material. Depicted here are a) axial strain and b) transverse strain.

V.2 Large Brazil tests with hole

The next set of experiments conducted were the "poker chip" Brazil tests. These tests were conducted on the "stock" un-pedigreed materials. As described in the work of Huang [2] it is possible to extract fracture toughness from the results of the Brazil test. In that work a disk with a pre-crack was further loaded until it produced crack extension. Based on sample dimension, applied load, and crack length the fracture toughness parameter could be calculated. Figure 4 depicts the way in which the calculation for fracture toughness is calculated. In our case the angle of loading would be 0°. Later work by Liu showed that the initial crack length could be variable [3]. In our present work the "pre-crack" was the existing hole in the center of the sample, however, since the loading process was captured for the image correlation technique, it would be possible to select any "frame" as the initial condition and measure the crack extension from that point, as long as the crack was growing stably. In addition to the previous work of using DIC to measure strain during a test, the technique of measuring damage using the correlation coefficient has been developed here at Los Alamos. In this process a baseline values for the undamaged sample is generated during early stages of sample loading. At some point during the sample loading a small location on the sample "loses" good correlation and from that point on the correlation of that point gets worse (a larger value). Typically, there is a very distinct transition in the correlation coefficient that can be associated to damaged material in one region and undamaged material in the other. By using the initial deviation, or "critical"

correlation valve the boundary of the damage zone can be determined. This is the method used to measure crack length and the time step between frames give the crack growth rate. A typical plot of the "maximum" correlation is shown in Figure 5. Generally, but not always, this value is associated with the same region of a sample (within a few pixels). In this example the development of the correlation coefficient with respect to time is shown along with a plot of the load displacement and correlation versus displacement for a polymer reinforced composite (High explosive). From these plots it can be seen how damage can be associated with the correlation coefficient. In our case the damage will be localized and easier to track but the technique will be the same.

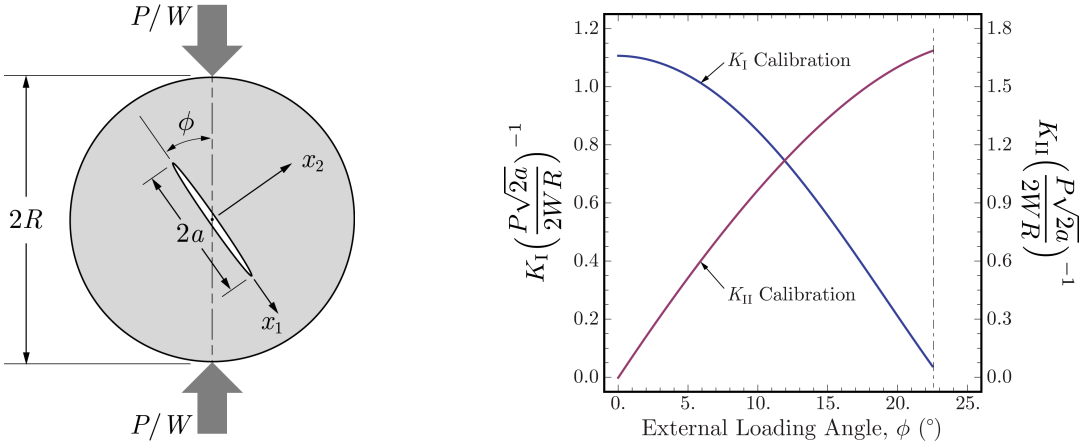

a) b)

Figure 4. Brazil disk characterization technique showing the a) sample geometry described in the development paper by Huang and b) the graph used to determine the fracture toughness modifier based on the off-axis loading angle of the preexisting crack.

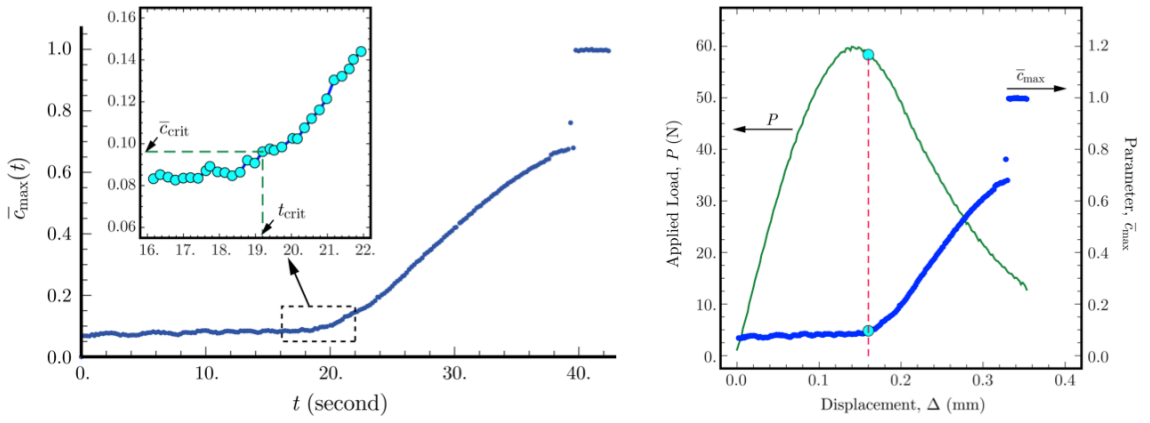

a) b)

Figure 5. a) Plot of the correlation coefficient versus time and b) plot of applied load and correlation coefficient versus displacement for a test on a polymer reinforced composite (high explosive material).

A much more extensive evaluation of the Brazil test was done in comparison to the tensile test because more information can be extracted from the test results. The summary of the applied load versus displacement for both DAP and seabreeze is shown in Figure 6. Two things to take

note of are the maximum load of the seabreeze was higher than that of DAP and the displacement at failure of the DAP was greater than that of the seabreeze indicating that seabreeze is stronger and more brittle than DAP.

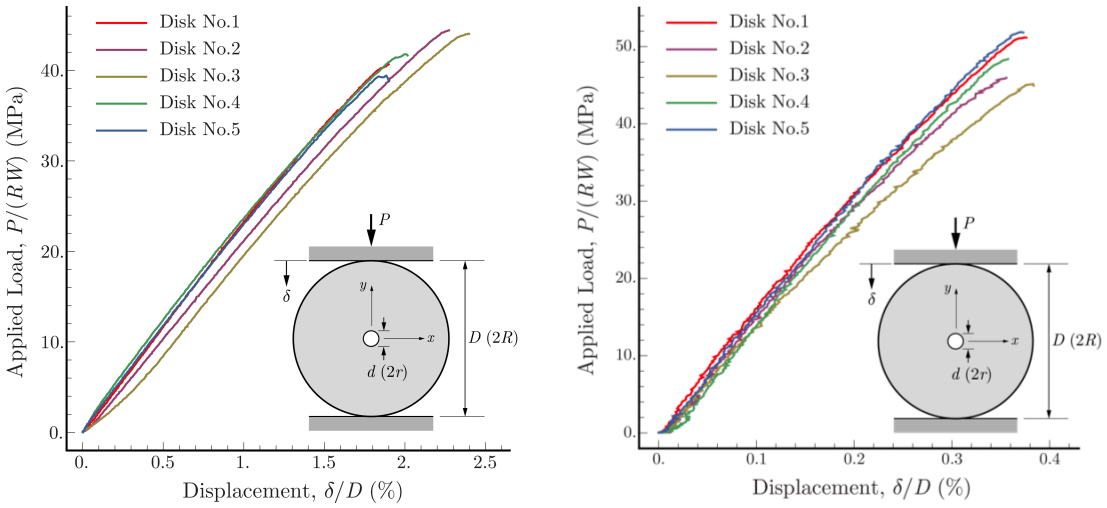

a) b)

Figure 6. Applied load versus displacement for a) DAP and b) seabreeze.

An evaluation of a typical DAP sample with the Brazil geometry using the DIC technique produces information for the deformation field evolution, the strain fields, the damage initiation location and time, and the progression of the crack boundary (using the correlation coefficient) (Figs 7-11). A plot of a typical load versus displacement curve for a DAP sample with specific points indicated is shown in Figure 7. The horizontal, vertical displacement fields and the calculated horizontal strain filed if presented in the next figure. (Fig. 8). It can be clearly seen that there are large displacement gradients (or strains) along the vertical diameter of the disc at both moments C and D. This concentrated deformation is a strong indication of the formation of damage and/or cracking prior to failure.

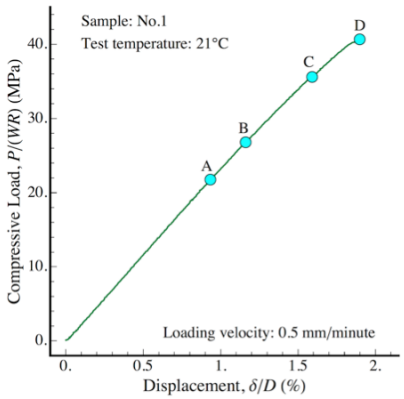

Figure 7. Load displacement curve for a typical DAP Brazil disk with a center hole. Points A to D represent different times during the loading process.

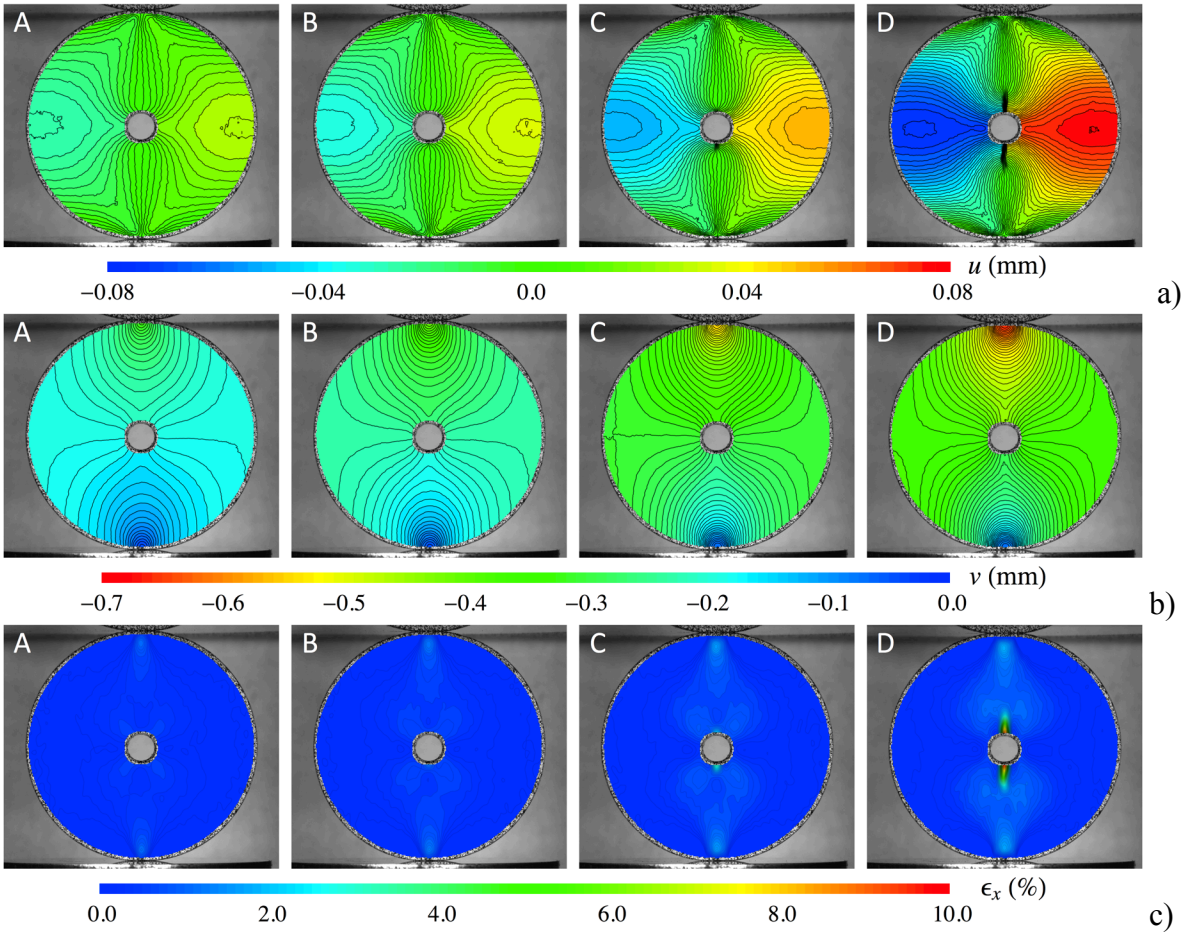

Figure 8. Images, marked with corresponding letters, associated with the moments in time indicated in Fig. 7. The top row, a), of images is for the horizontal displacement. The middle row, b), is for vertical displacement fields and c) are calculated horizontal strain fields derived from the displacements.

As mentioned earlier in this section, it is possible to determine the time and location when damage initiates in each sample (Fig.9). Based on the quantitative analysis of the correlation coefficient value it has been determined the critical moment in time when localization occurred (for sample No.1) was at time B and unstable fracture happened at moment D (Fig. 10). The same notation has been used when doing the analysis of each sample and there is a uniques plot for these parameters for each sample. Figure 9 is a graph of the maximum correlation value, or least accurate comparison between images. This value is not specifically related to a single point but once a crack is initiated the correlation value of that point will increase rapidly and this curve can be thought of as an accurate representation correlation coefficient at the damage initiation site. Typically, the maximum correlation value is associated with the region, if not exact position, of the onset of damage and the perimeter of the damage region can be traced when the value of correlation exceeds the critical correlation value. From plots shown in Figures 9 and 10 one can see how the correlation value tracks with the load displacement plot. The sequential strain fields are shown in Figure 11 for the different reference points shown on Figure 10 with the damage zone indicated by the red outline initiating vertically from the hole. These images relate the damage in the sample to the length of the crack or crack opening at the hole.

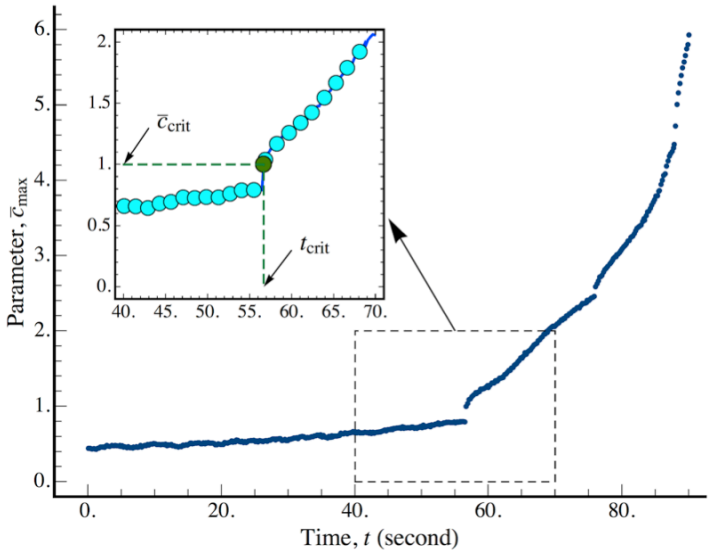

Figure 9. Plot of the correlation coefficient versus time for sample No. 1. This plot will be unique for each sample.

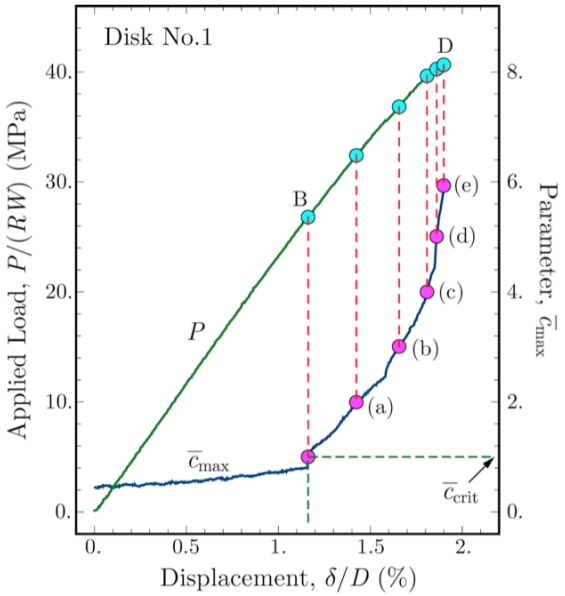

Figure 10. Plot of applied load and correlation coefficient versus displacement for sample No.1

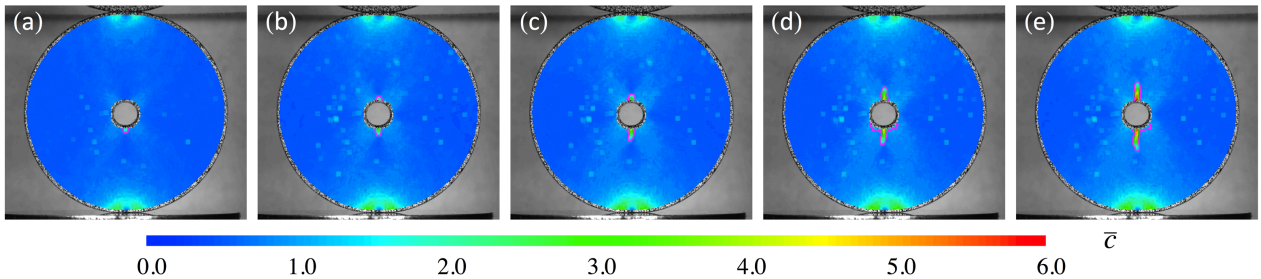

Figure 11. Sequential horizontal strain field maps for sample No.1 showing the evolution of the main cracks. These maps are referenced to (a) through (e) in Fig. 10.

Seabreeze was characterized in a very similar manner and shows similar trends. However, the primary differences between the two materials is that seabreeze is much stiffer and the deformation before failure is much less than the DAP material. This is not a statement of comparison but one of restriction. Figure 12 and 13 shows the load versus displacement plot and the associated displacement and strain fields for seabreeze (Sample No1), respectively. The magnitude of the displacement is much smaller and there is much less crack growth seen before failure in the seabreeze material when compared to DAP. The plot of the correlation coefficient (Fig. 14) shows not only a rapid change in the parameter but also a very limited number of images to analyze before the failure event occurs. Also notice that the magnitude of this value is much smaller that those found in the DAP materials. An image of the final strain field for sample (Fig. 15) No. 1 indicates a relatively long crack but there is only a very brief period of time when damage is observed before the sample fails. In reality there would be only a single image to analyze and there would be no way of knowing how the bluntness of the hole influenced crack growth so a measurement of fracture toughness using this test was not completed.

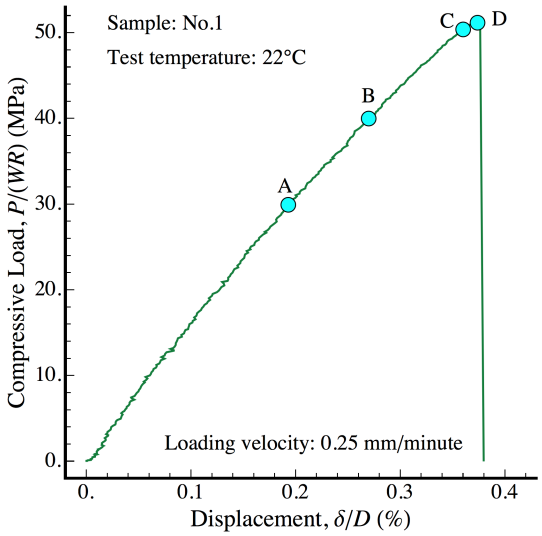

Figure 12. Load displacement curve for a typical seabreeze Brazil disk with a center hole. Points A to D represent different times during the loading process.

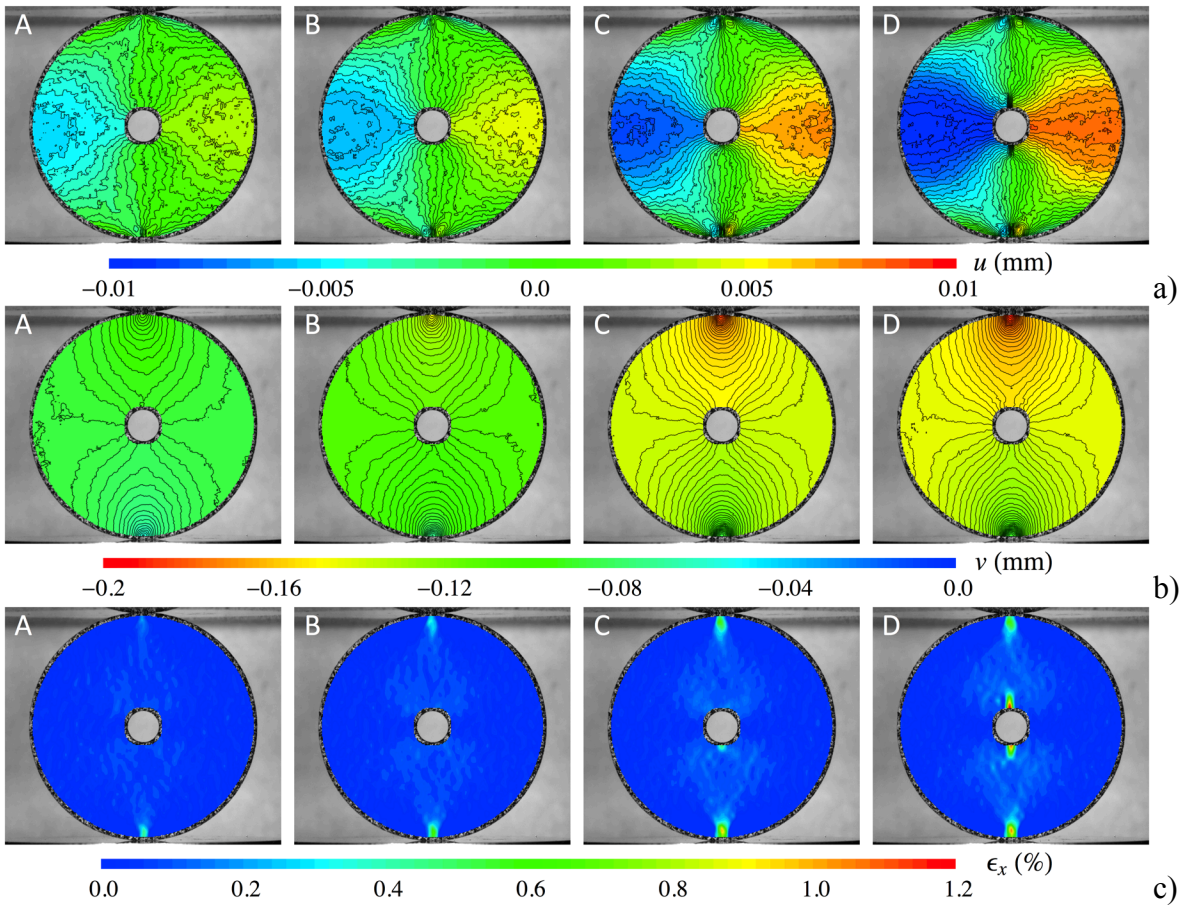

Figure 13. Images, marked with corresponding letters, associated with the moments in time indicated in Fig. 12. The top row, a), of images is for the horizontal displacement. The middle row, b), is for vertical displacement fields and c) are calculated horizontal strain fields derived from the displacements.

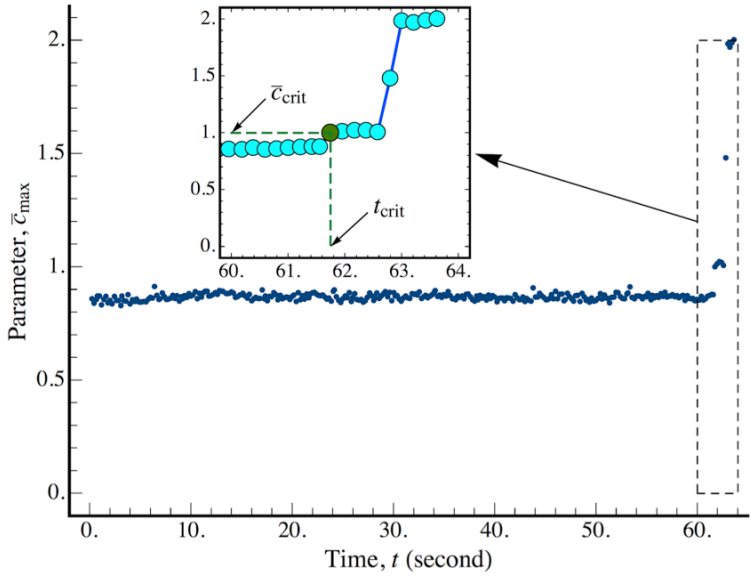

Figure 14. Plot of the correlation coefficient versus time for sample No. 1. This plot will be unique for each sample.

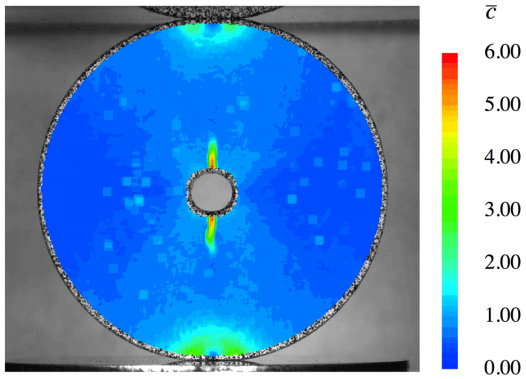

Figure 15. Horizontal strain field map for sample No.1 showing the final image prior to failure with the correlation scale show on the side.

V.3. Small Brazil disks without hole

In order to verify that the center hole did not influence the results of the Brazil tests the small Brazil test geometry was investigated. These samples were machined from the "poker chips" and therefor had a size limitation. The analysis of these samples was limited, but two things to make note of are the applied load of the sample was nearly three time larger for the small disk when compared to the large disk implying that the hole probably acted like a pre crack. Along the same line of reasoning is the fact that the relative displacement to failure of the DAP was also five times larger in the smaller disk also indicating that the hole influenced the crack initiation. It was also observed that when these samples failed it happened quite rapidly and no images of the failure event were captured. Again this is not unexpected because the stored energy in the system could be released very rapidly once the crack initiated. The same observations can be made about the seabreeze material but the magnitude of the load difference was only two and the relative displacement was also only two time larger than the larger disk having a hole.

The following plots and figures summarize the work on the small disk samples. Figure 16 are summary plots of the load versus displacement for the DAP and seabreeze materials. The next figure shows an individual curve of the load versus displacement for the two materials (Fig. 17). Figures 18 and 19 show the evolution of the horizontal and vertical displacement fields for DAP and seabreeze, respectively. The next two figures show corresponding strain fields for axial, transverse and shear strains. (Figs. 20, 21) also for DAP and seabreeze. In these tests it is important to notice that the strains and damage are concentrated at the loading surfaces, not in the center of the disks. Therefore, the two types of Brazil tests really do not show the same type of damage nucleation or growth. Also because there is quite a bit more stored energy in the smaller Brazil disks the fracture occurred at a much faster rate and crack growth could not be measured.

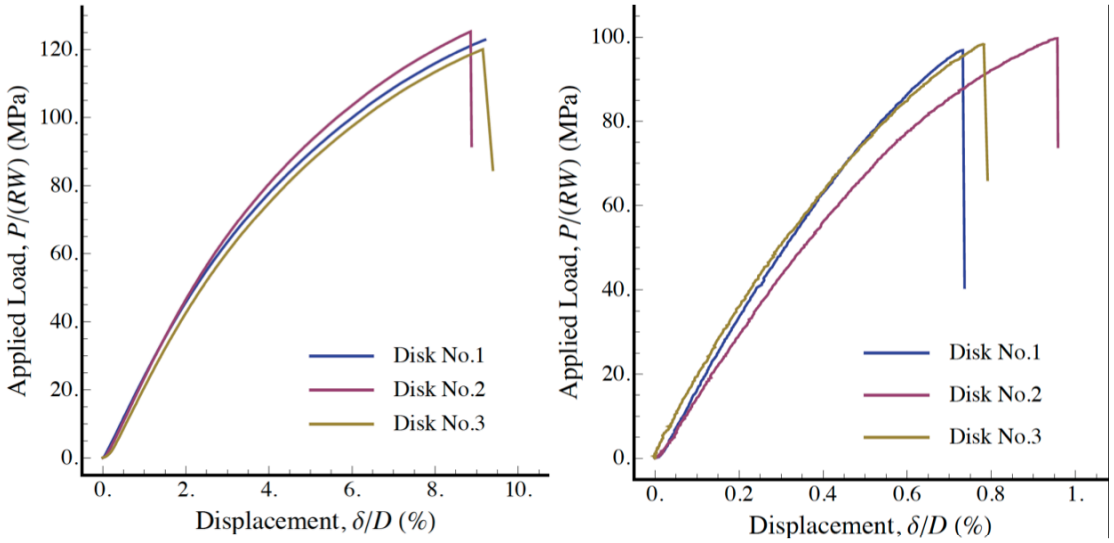

Figure 16. Applied load versus displacement for small Brazil disks for a) DAP and b) seabreeze.

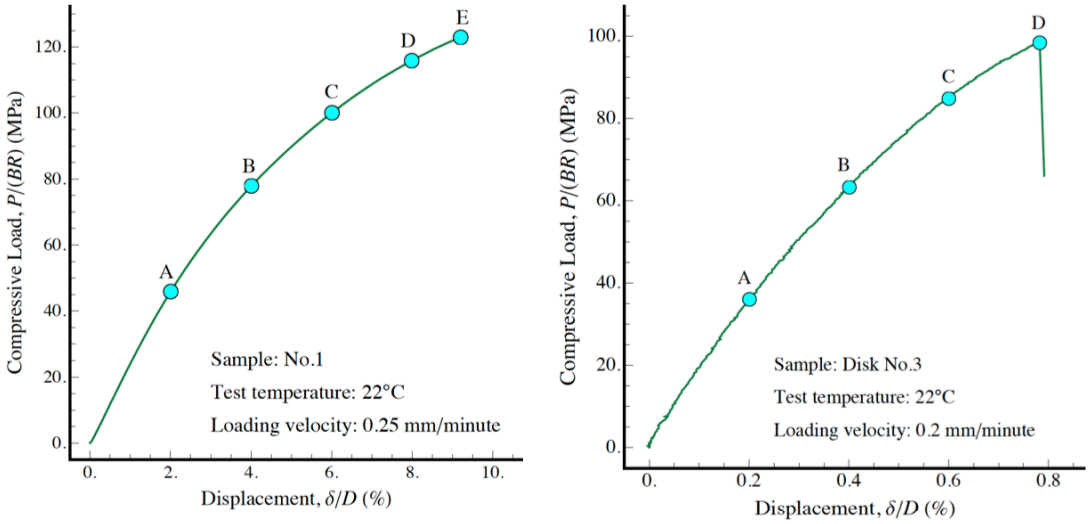

Figure 17. Typical load displacement curve for a small Brazil disk. Points A to E for a) DAP and A to D for b) seabreeze representing different times during the loading process.

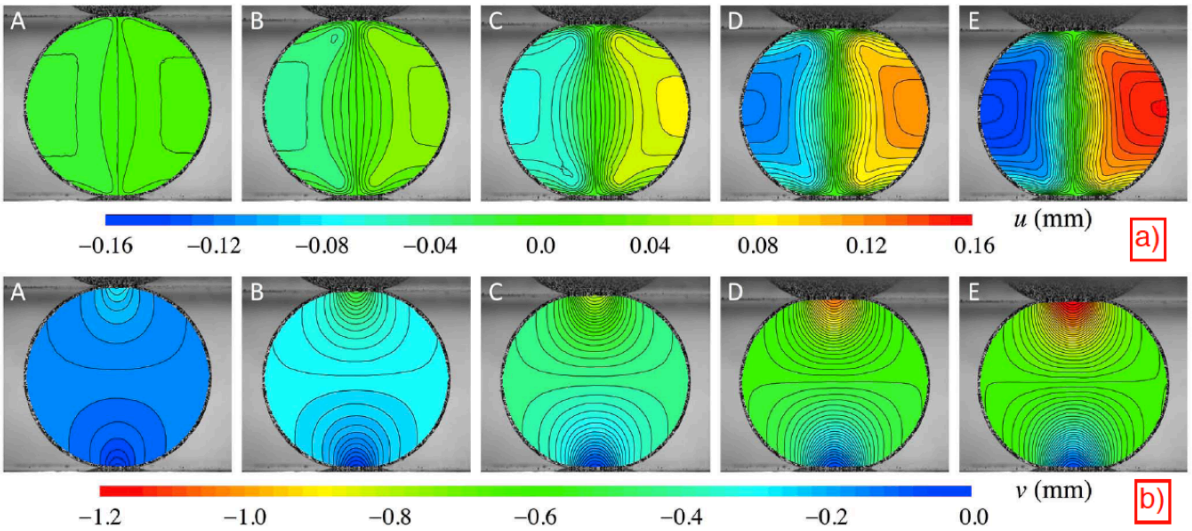

Figure 18. Images, marked with corresponding letters, associated with the moments in time indicated in Fig. 17a for DAP. The top row, a), of images is for the horizontal displacement. The second row, b), is for vertical displacement fields.

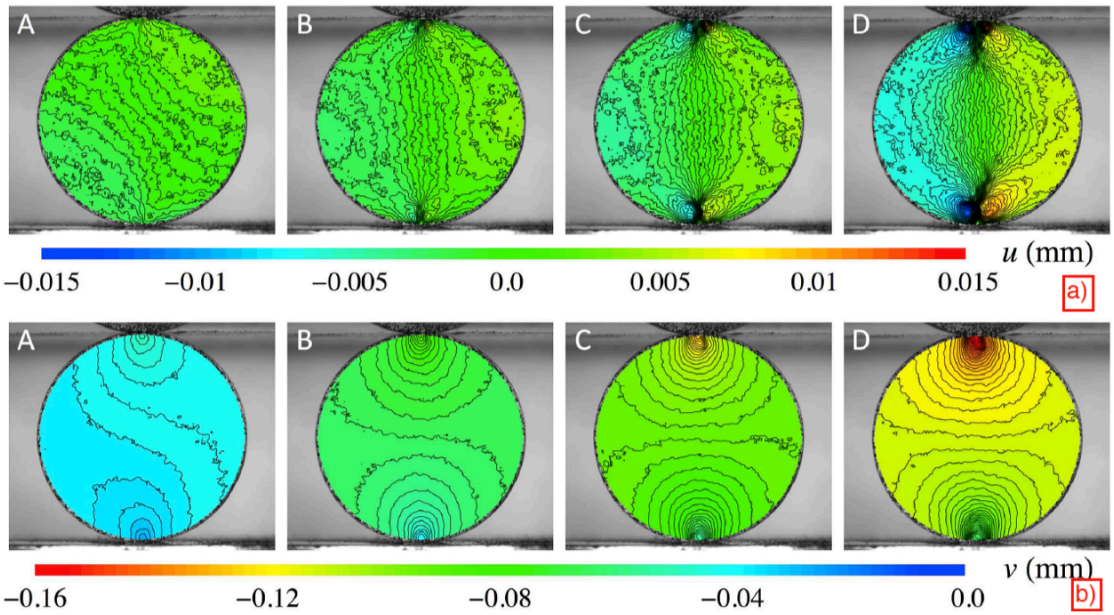

Figure 19. Images, marked with corresponding letters, associated with the moments in time indicated in Fig. 17b for seabreeze. The top row, a), of images is for the horizontal displacement. The second row, b), is for vertical displacement fields.

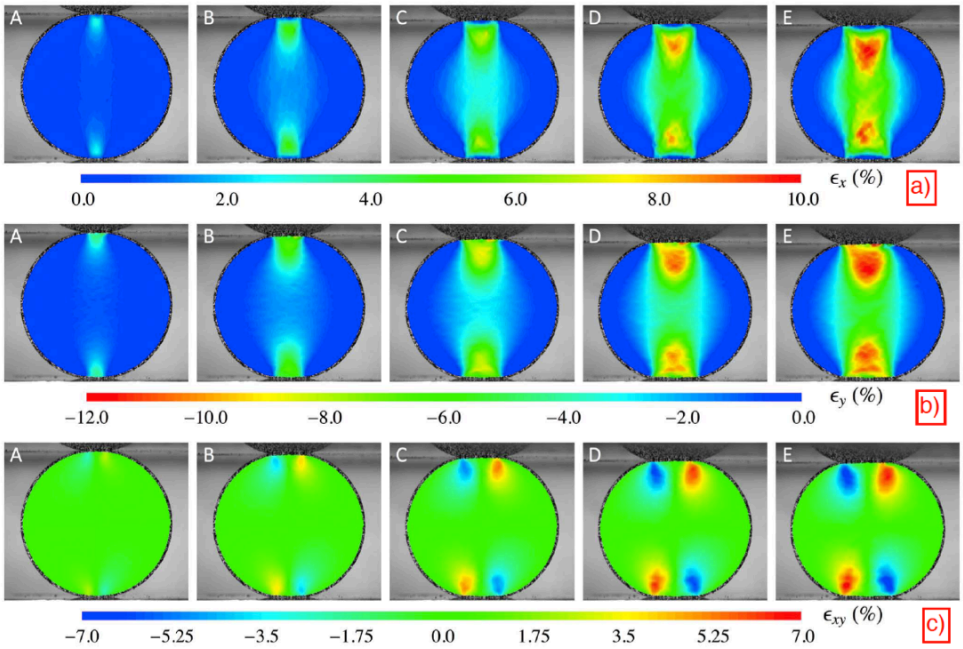

Figure 20. Images, marked with corresponding letters, associated with the moments in time indicated in Fig. 17a. The top row, a), of images is for the calculated horizontal strain fields. The middle row, b), is for calculated vertical strain fields and c) are calculated shear strain fields derived from the displacements.

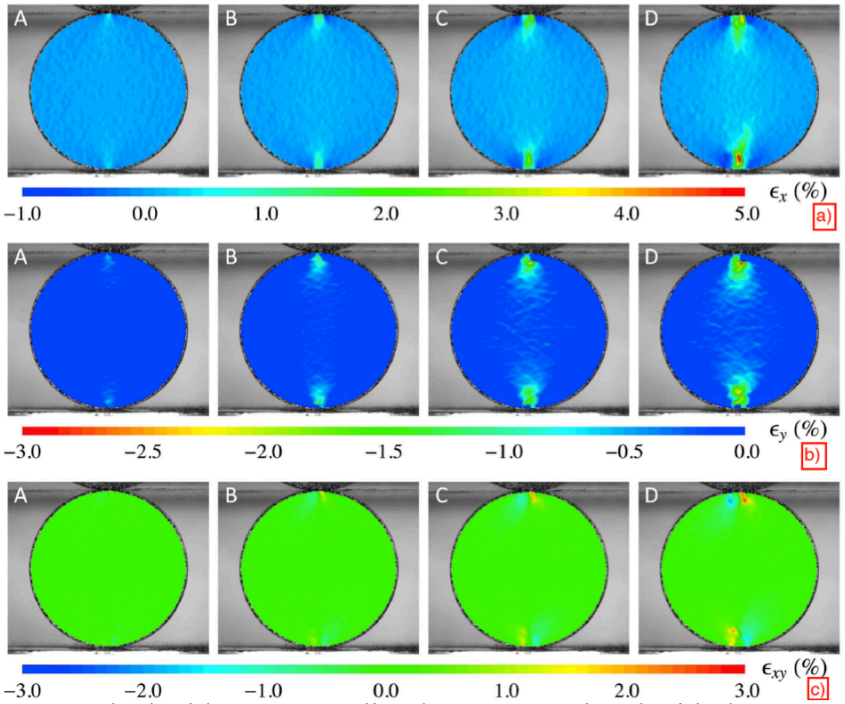

Figure 21. Images, marked with corresponding letters, associated with the moments in time indicated in Fig. 17b for the a) calculated horizontal strain fields, b) calculated vertical strain fields and c) calculated shear strain fields derived from the displacements.

V.4. “Compression-Fracture”

It was determined that a new specimen geometry was needed to try to generate a controlled crack growth in the seabreeze material based on the earlier results obtained from the Brazil test. The "compression-fracture" specimen fracture geometry was first investigated on the DAP material by machining rectagular specimens with a center hole from non-pedigreed "poker chip" disks described in section 4. Two tests were performed in the un-aged non-pedigreed DAP material to confirm that slow crack growth would be achieved. Following that un-aged but pedigreed samples were tested for both DAP and seabreeze. Other samples were placed in an oven at 90°C for approximately 120 days. Tables 1 (DAP) and 2 (seabreeze) show the test geometries for the two materials evaluated. All of the seabreeze samples for this geometry came from pedigreed material. The "Un-aged Ped" and "DPO" oven aged DAP samples came from pedigreed sources. Samples labeled as "Block0X" and "U-1" refer to un-aged samples. "SB" samples refer to the larger oven aged seabreeze samples. The larger block geometry was used on the more brittle material to help control the crack growth by using a greater area. This sample modification was made due to experiences learned in the "poker chip" characterization where the thin seabreeze samples fractured quite rapidly.

Table 1 DAP Compression-Fracture sample dimensions

Sample Name	*H* (mm)	*W* (mm)	*B* (mm)	*d* (mm)
Unped 1	28.8531	12.7159	3.208	3.6690
Unped 2	28.8563	12.7921	3.218	3.6659
Block 3	28.2296	9.5758	4.8622	3.1566
Block 4	28.2264	9.5796	4.7663	3.1807
Aged Unped 1	29.220	12.762	3.190	3.773
Aged Unped 2	29.270	12.771	3.158	3.654
Aged Unped 3	29.200	12.753	3.161	3.644
Un-aged Ped-3	29.644	9.521	4.690	3.043
Un-aged Ped-4	29.603	9.541	4.686	3.109
DPO-1-1	29.693	9.530	4.683	3.034
DPO-1-2	29.610	9.526	4.687	3.035
DPO-2-1	29.682	9.547	4.683	3.063
DPO-2-2	29.627	9.549	4.770	3.067
DPO-3-1	28.011	9.522	4.681	3.037
DPO-3-2	30.128	9.516	4.794	3.096

Table 2 Seabreeze Compression-Fracture sample dimensions

Sample Name	*H* (mm)	*W* (mm)	*B* (mm)	*d* (mm)
Block01	24.7447	9.5606	9.6514	3.0797
Block02	25.3740	9.5574	9.5898	3.0550
Block03	25.0234	9.5148	9.6342	3.0861
Block04	24.8844	9.4755	9.6234	3.2328
Block05	24.7910	9.5472	9.6279	3.2817
U-1	24.825	9.507	9.502	3.130
SB-2-1	24.889	9.527	9.566	3.128
SB-2-2	25.456	9.520	9.519	3.115
SB-2-3	24.839	9.489	9.561	3.106
SB-3-1	24.872	9.452	9.514	3.097
SB-3-2	25.427	9.621	9.574	3.101
SB-3-3	24.822	9.488	9.549	3.106

The load displacement response of the un-aged DAP is shown in Figure 22. In this plot the two "blue" curves are from un-pedigreed materials. They fall between the tested pedigreed samples. The curves are essentially the same during the loading process meaning that the pedigreed and un-pedigreed materials behave similarly. A plot of the aged DAP samples is seen on the next plot (Fig. 23). The un-pedigreed materials tend to fall at the higher end of the failure strength range when comparing the source of the material. A final comparison is a plot of the un-aged versus aged samples (Fig. 24). The aged material has a slightly lower loading slope for both un-pedigreed and pedigreed materials, but both cases there is overlap of the data implying that aging does influence the mechanical behavior but not dramatically.

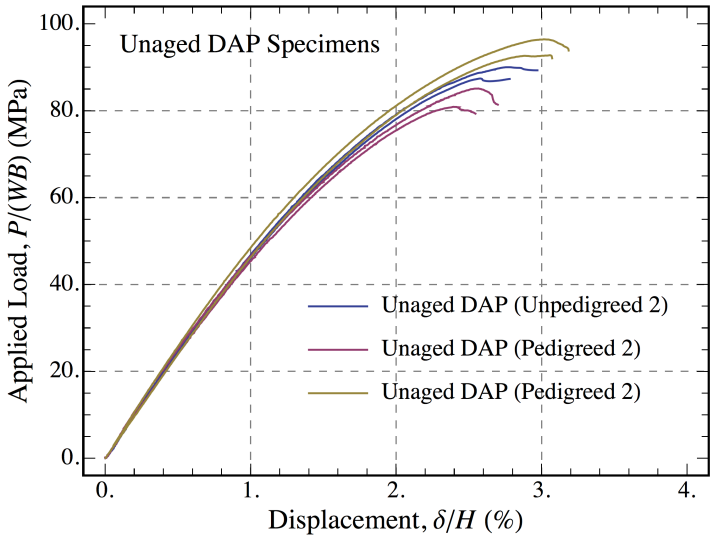

Figure 22. Load displacement plot for un-aged DAP materials. Notice that the un-pedigreed material is nominally the same a the pedigreed material.

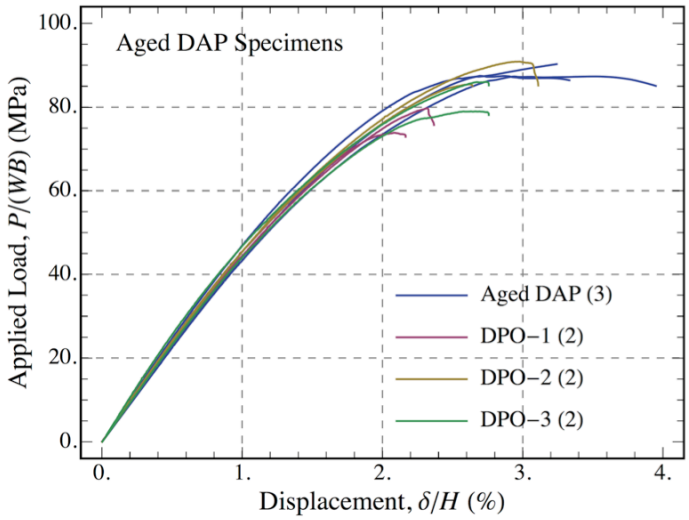

Figure 23. Load displacement plot for aged DAP materials. Again, the un-pedigreed material is nominally the same as the pedigreed material.

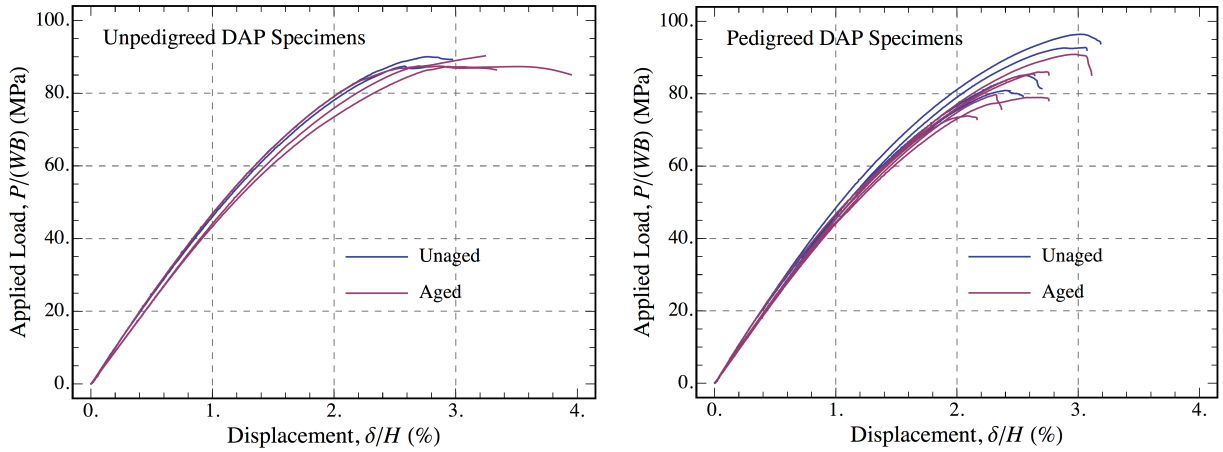

Figure 24. Load displacement plot for DAP materials comparing the effect of aging for the a) un-pedigreed material and b) pedigreed material.

The intension of this geometry was to be able to generate crack growth in the test sample that is slow enough to capture images during deformation in order to measure crack growth rates. Again a plot of the load displacement curve (Fig. 25) for a typical un-pedigreed sample is shown with indicators showing times when corresponding strain field maps are presented (Fig. 26). Using the technique to determine the correlation coefficient it is possible to determine the time and location when damage initiates for this sample geometry on the DAP material confirming that this technique will work just as well as the Brazil test with a hole for a rigid polymer (Fig.27). The same notation has been used when doing the analysis of each sample and there is a unique plot for these parameters for each sample. Again, the critical correlation coefficient will be used to track the boundary of the "damaged" region showing where the crack is located and the rate at which it grows. The maximum correlation value is not specifically related to a single point but once a crack is initiated the correlation value of that point will increase rapidly and this curve can be thought of as an accurate representation correlation coefficient at the damage initiation site. Typically, the maximum correlation value is associated with the region, if not exact position, of the onset of damage and the perimeter of the damage region can be traced when the value of correlation exceeds the critical correlation value. Using the same technique described in earlier sections it is possible to determine the damage initiation time (displacement). Plots for the un-aged and aged damage initiation displacement are presented in Figure 28. A summary plot showing just the damage initiation stress versus cross head displacement is presented on next figure (Fig. 29). The information that is important to pull off of this plot is that all the damage initiation versus displacement seems to fall on a line. This implies that the modulus of both the aged and un-aged materials seem to be identical and that aging the material does not seem to affect fracture toughness significantly. This result is in agreement with the observations made about Figure 24 where the aged materials were seen to be very slightly less stiff than the un-aged samples. Plots showing similar results for the pedigreed material are presented in Figures 30 to 33.

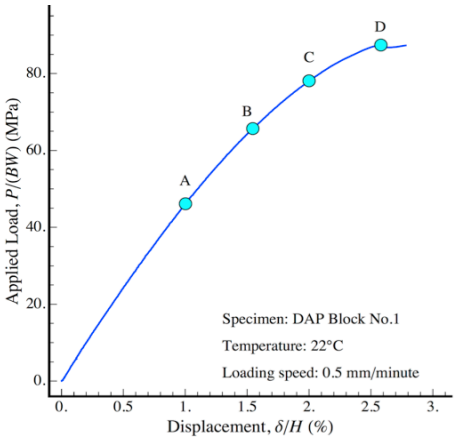

Figure 25. Load displacement curve for a typical unpedigreed DAP compression fracture sample.

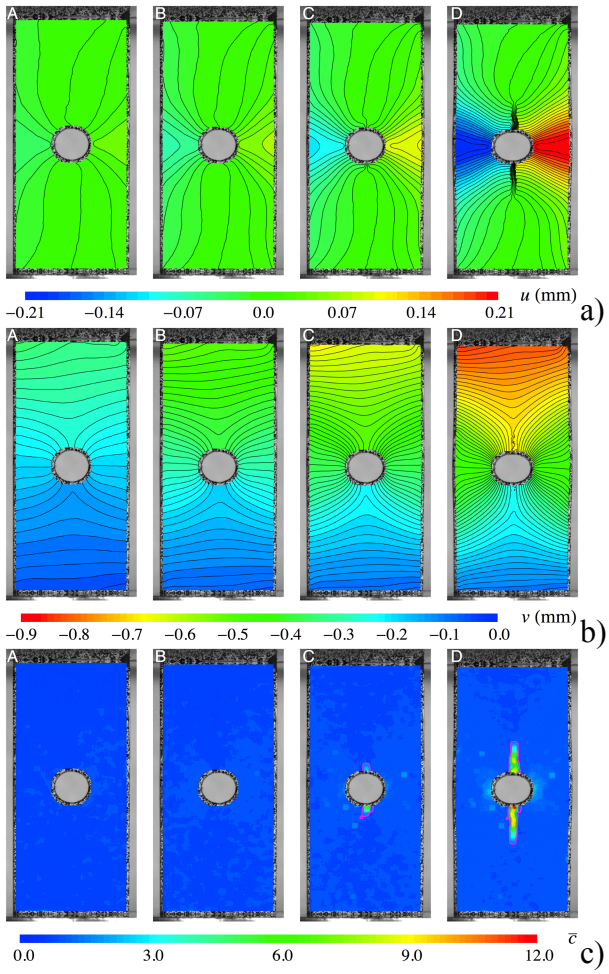

Figure 26. Images, marked with corresponding letters, associated with the moments in time indicated in Fig. 25. The top row, a), of images is for the horizontal displacement. The middle row, b), is for vertical displacement fields and c) are calculated horizontal strain fields derived from the displacements.

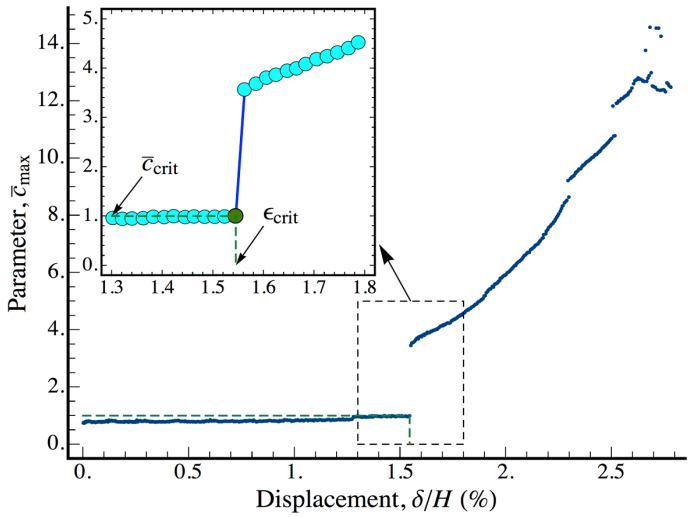

Figure 27. Plot of the correlation coefficient versus time for un-aged, un-pedigreed sample 1. This plot will be unique for each sample.

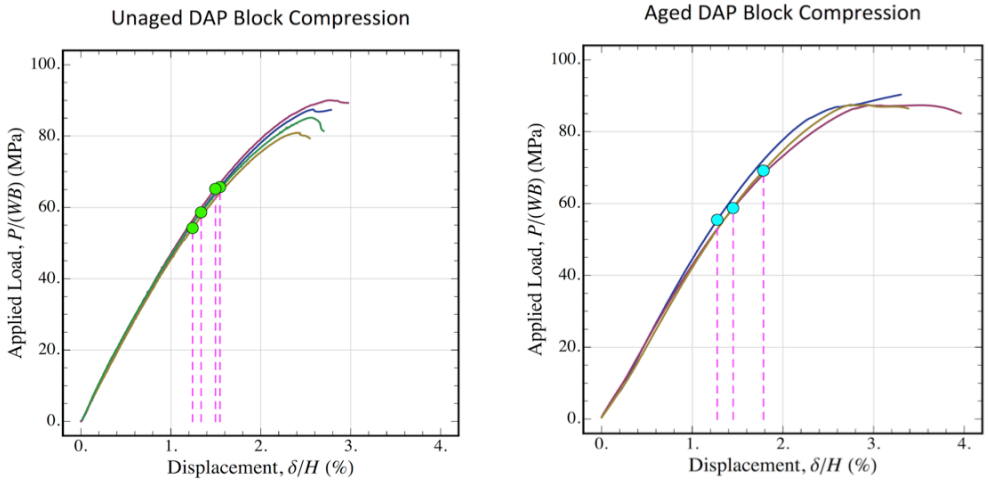

Figure 28. Damage initiation for a) un-aged and b) aged DAP samples.

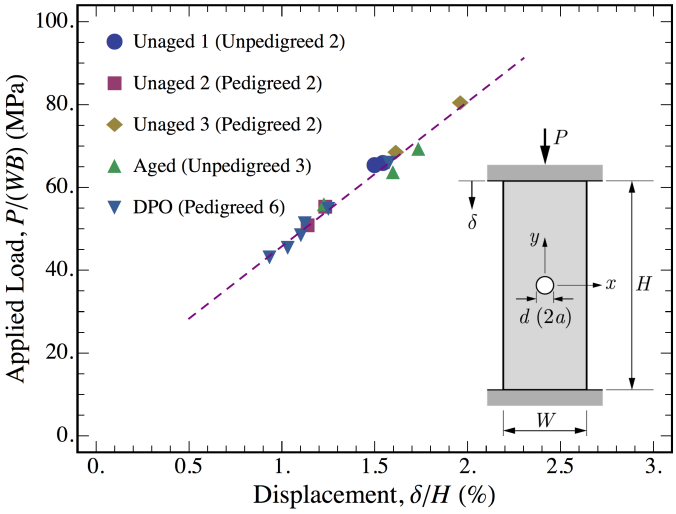

Figure 29. Plot of the Damage initiation value for all DAP samples.

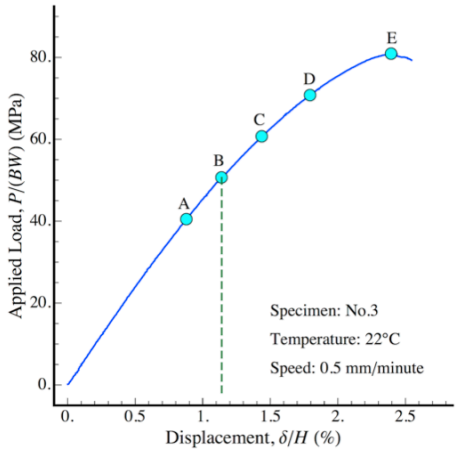

Figure 30. Load displacement curve for a typical pedigreed DAP compression fracture sample (Block No.3). Location B is the moment when the correlation value begins to change rapidly.

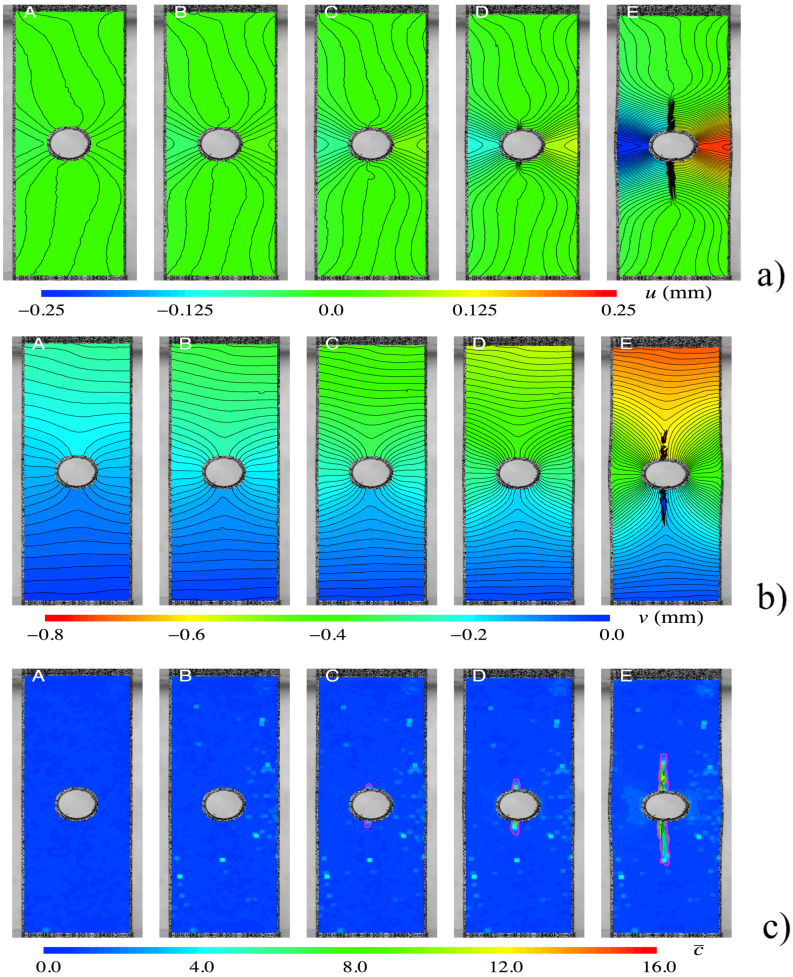

Figure 31. Images, marked with corresponding letters, associated with the moments in time indicated in Fig. 30. The top row, a), of images is for the horizontal displacement. The middle row, b), is for vertical displacement fields and c) a map of the correlation coefficient.

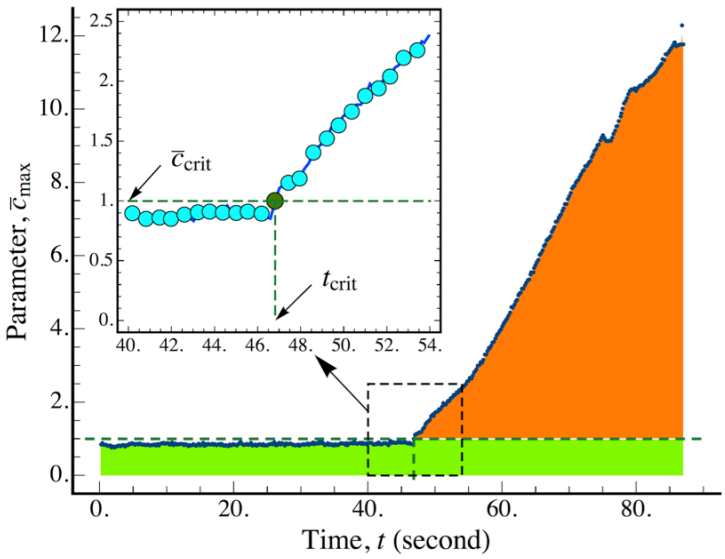

Figure 32. Plot of the correlation coefficient versus time for un-aged, pedigreed specimen No.3. This plot will be unique for each sample.

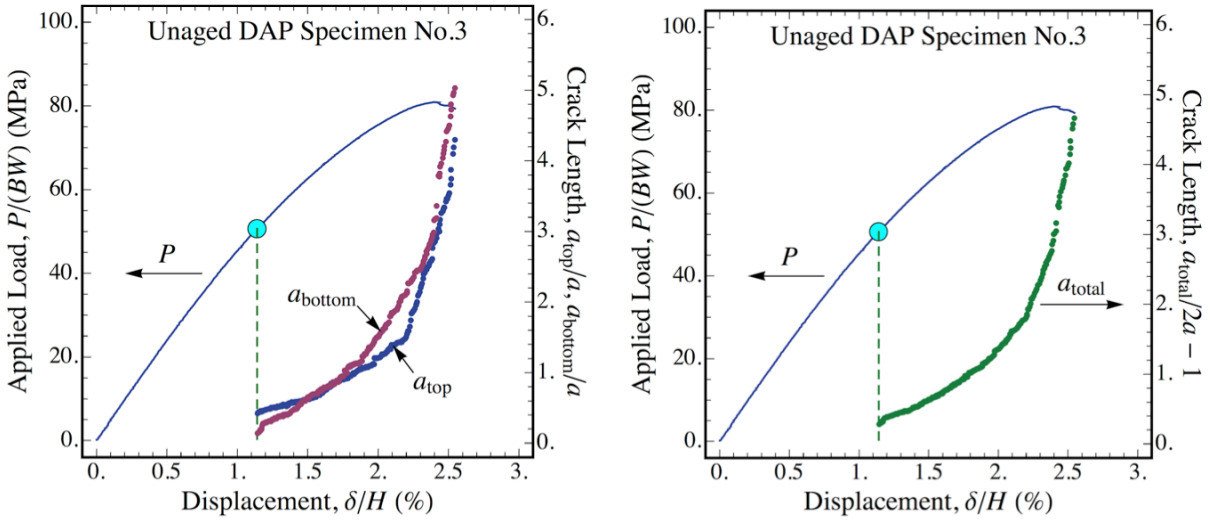

Figure 33. Plot of applied load and correlation coefficient versus displacement for Block No. 3. Plot a) is for the cracks shown individually and plot b) is when the lrack lengths are added together.

Although the compression fracture geometry was demonstrated to work well for the DAP materials, testing of the seabreeze block samples would determine if this geometry would be suitable for uses on more brittle materials. The data will be presented in the same manner as for the DAP compression fracture tests. Figures 34 to 36 present the data collected for the seabreeze tests that were run.

The load displacement response of the un-aged seabreeze is shown in Figure 34. In this plot the five “blue” curves are from pedigreed materials. The differences between the plots as shown are because of imperfections in the loading ends of the sample. After an initial load that shows that the samples ends were not parallel the rate of loading, or modulus, seems to increase at nominally the same rate. This means that the un-pedigreed and pedigreed materials are nominally

the same. A plot of the aged seabreeze samples is seen on the next plot (Fig. 35). There was less scatter in the data than in the unaged samples indicating better quality of sample. A final comparison is a plot of the un-aged versus aged samples (Fig. 36). The two materials have a slightly lower loading slope for both un-pedigreed and pedigreed materials, but both cases there is overlap of the data implying that aging does influence the mechanical behavior but not dramatically. One item to make note of is that the first pedigreed seabreeze samples were inadvertently machined with water, and subsequently dried at 40°C for several days. This error in processing does not seem to have changed the material response.

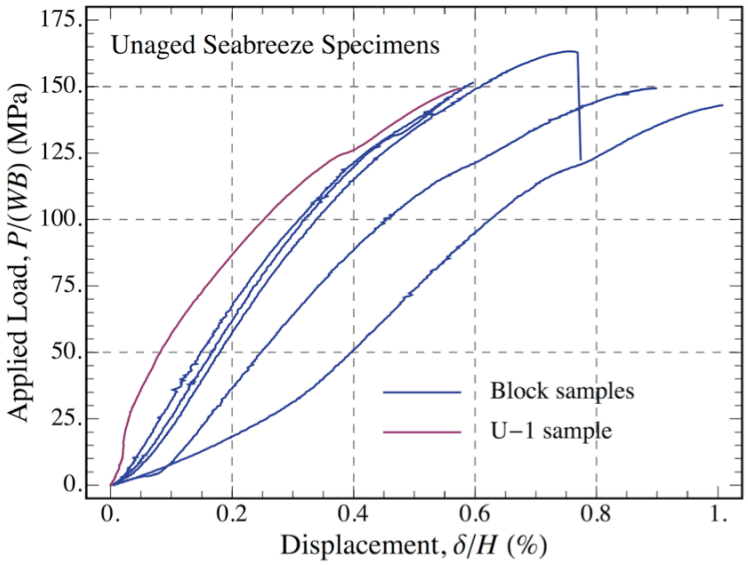

Figure 34. Load displacement plot for un-aged seabreeze materials. Notice that the un-pedigreed material is nominally the same as the pedigreed material with differences due to machining defects.

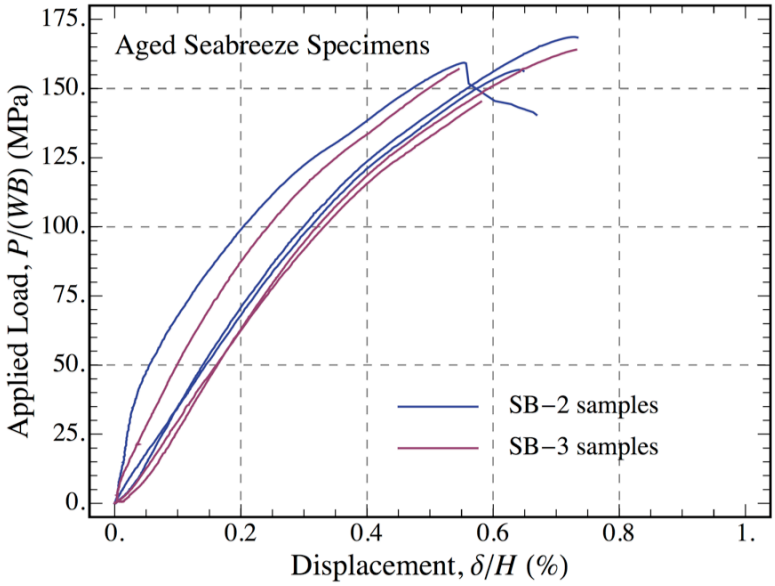

Figure 35. Load displacement plot for aged seabreeze materials. Only pedigreed materials were aged.

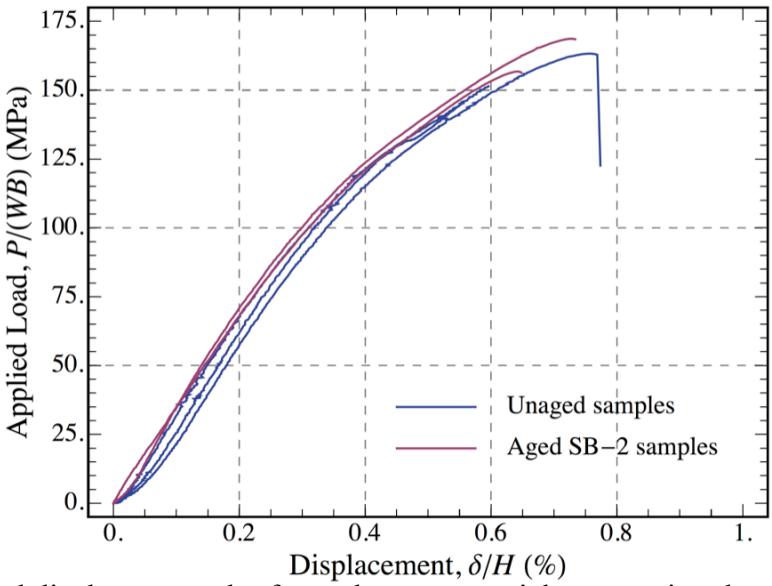

Figure 36. Load displacement plot for seabreeze materials comparing the effect of aging for the pedigreed material.

This technique has been shown to work well for the seabreeze material and the following plots show the analysis of the test data. A plot of the correlation coefficient for the seabreeze material is shown in Figure 37. Each test uses the same type of analysis and similar plots are generated for each test. The critical correlation coefficient is used in the same way as described above. A summary plot showing just the damage initiation stress versus cross head displacement is presented on next figure (Fig. 38). The information that is important to pull off of this plot is that all the damage initiation versus displacement seems to be at approximately the same value (~100 MPa). This seems to indicate that the "critical flaws" are well distributed and relatively small allowing the material to initiate damage (from the hole) at approximately the same stress. There was one outlier as far as displacement and damage were concerned and I believe that it is associated with a sample geometry issue.

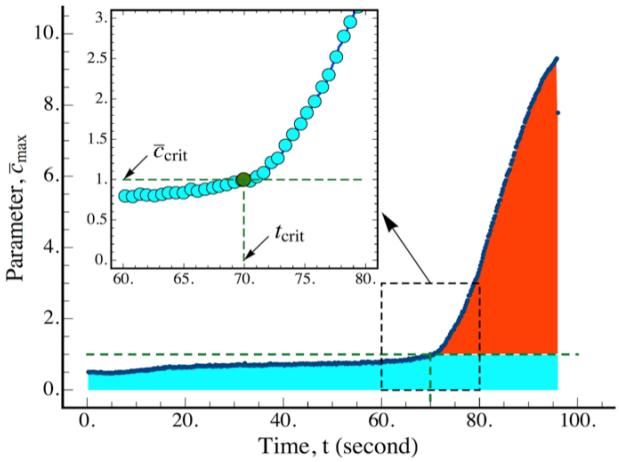

Figure 37. Plot of the correlation coefficient versus time for un-aged, pedigreed sample 1. This plot will be unique for each sample.

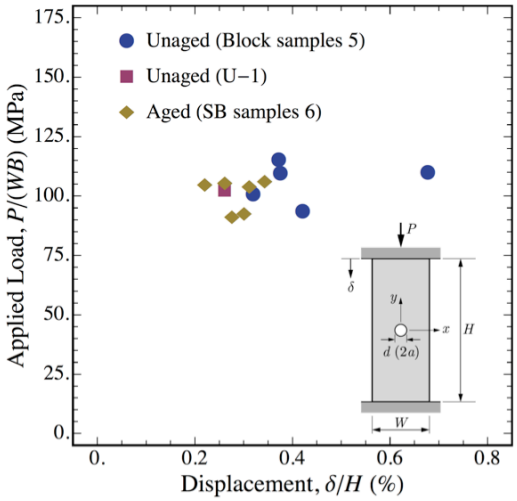

Figure 37. Plot of the Damage initiation value for all seabreeze samples.

VI. Fracture toughness Calculations

The fracture toughness, or critical stress intensity factor of the Brazil disk with a hole was calculated from the equation:

$$K_{\mathrm{IC}} = 1.1065\left(\frac{P_{\mathrm{crit}}}{WR}\cdot\frac{\sqrt{2a}}{2}\right) \tag{1}$$

Where P_{crit} is the load at failure, W is the width of the sample, R is the radius of the disk and *a* is the crack length. The constant, 1.1065 comes from the mode 1 critical stress intensity factor calibration curve. The plot for K_{1C} for the 5 tests test run on un-pedigreed DAP is shown in the next figure. (Fig. 38). This graph shows reproducible results for this test geometry and gives an average value of 3.21 MPa$\sqrt{m}$.

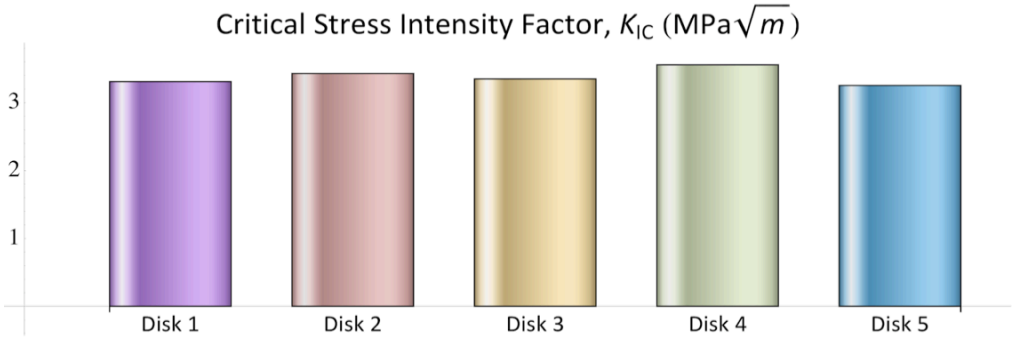

Figure 38. Critical stress intensity factor for DAP Brazil disks with a center hole.

The critical stress intensity factor for the compression-fracture spacimen is derived from the following equation. It has been modified to reflect the fact that the crack lengths may be different as they propagate from the center hole toward the top and bottom of the test sample. In this case the initial hole diameter is *a*, the stress is the far field stress and is found by dividing the applied load by the loading area (width x thickness). a_{top} and a_{bottom} are the crack length propagating from the top and bottom of the hole respectively.

$$K_{\mathrm{IC}} = -\left(\frac{a_{\mathrm{top}} + a_{\mathrm{bottom}}}{2a}\right)^{1/2} \left\{ \frac{1.1}{\left(1 + \frac{a_{\mathrm{top}} + a_{\mathrm{bottom}}}{2a}\right)^{3.3}} \right\} \sigma\sqrt{\pi a} \qquad (2)$$

Using the equation above a calculation of the stress intensity factor as a function of crack length was calculated assuming that the stress applied is equal to the applied load divided by the width and thickness of the sample at the contact surface (Fig. 39). The solution for the stress intensity factor is a semi-empirical in formula used to calculate the fracture toughness on a PMMA plate. We have applied the technic as best we could to analyze our test results.

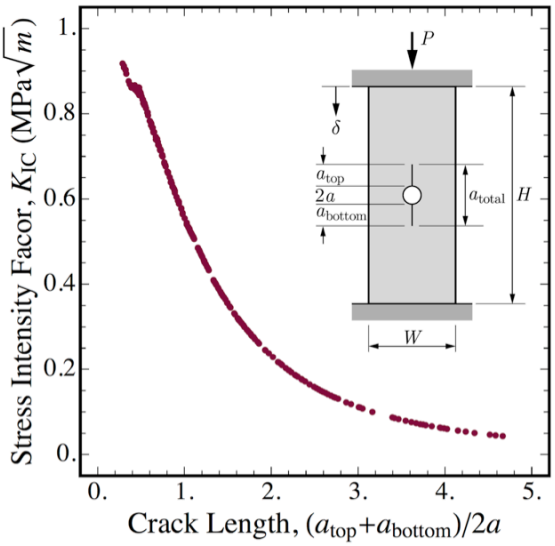

Figure 39. Critical stress intensity factor for DAP compression fracture sample with a center hole.

It is important to note that this experimental technique does not give a single value for the stress intensity factor. It does, however, show how crack growth and mechanical response to loading are correlated. Also, because the stress intensity factor is so closely tied to crack growth and our hypothesis that this property is most influenced by aging any ways of showing differences in behavior have great value. The following plots show the fracture toughness values for un-aged DAP (Fig. 40) and aged DAP (Fig. 41) for both pedigreed and un-pedigreed samples. These curves represent the stress intensity factors for a growing crack.

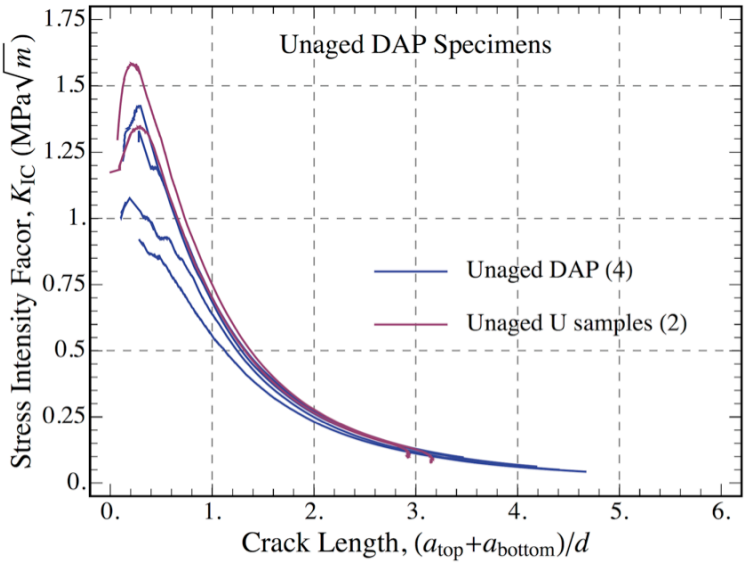

Figure 40. Summary plot for the critical stress intensity factor for un-aged DAP compression fracture sample with a center hole. This plot shows results for both un-pedigreed and pedigreed materials.

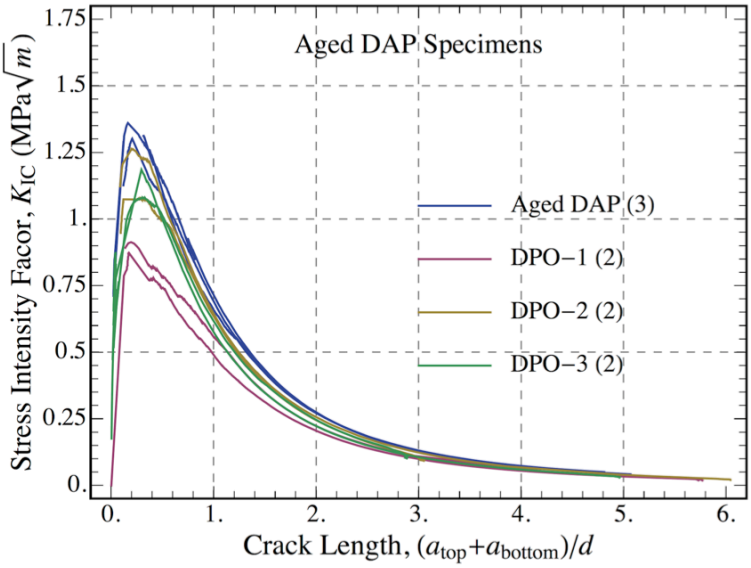

Figure 41. Summary plot for the critical stress intensity factor for aged DAP compression fracture sample with a center hole. This plot shows results for both un-pedigreed and pedigreed materials.

Although there are outliers to the test results it can be generally said that the tests are repeatable and that the general trend in fracture toughness is consistant with results seen for the Brazil geometry. Generally, it can be concluded that the fracture toughness for aged materials is lower than that of the un-aged material and this is true for both the unpedigreed and pedigreed materials. The plot below shows the results for the pedigreed DAP material (Figs. 42)

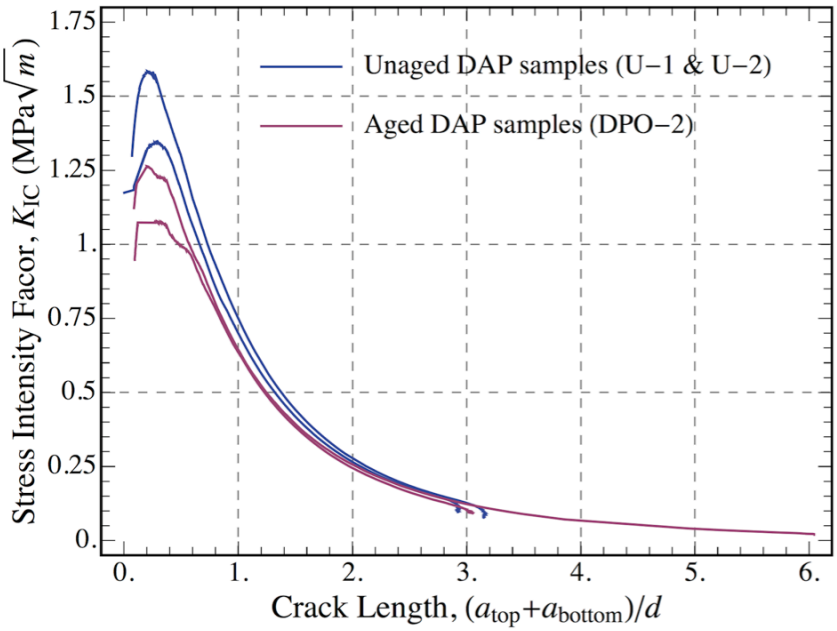

Figure 42. Comparison plot for the critical stress intensity factor for pedigreed DAP in both un-aged and the aged condition for the compression fracture sample with a center hole.

Similar plots for the seabreeze materials are presented in the next three plots. The first one shows the stress intensity factor for the un-aged material (Fig. 43). Note that some of these samples were machined wet but they were all taken from a pedigreed source.

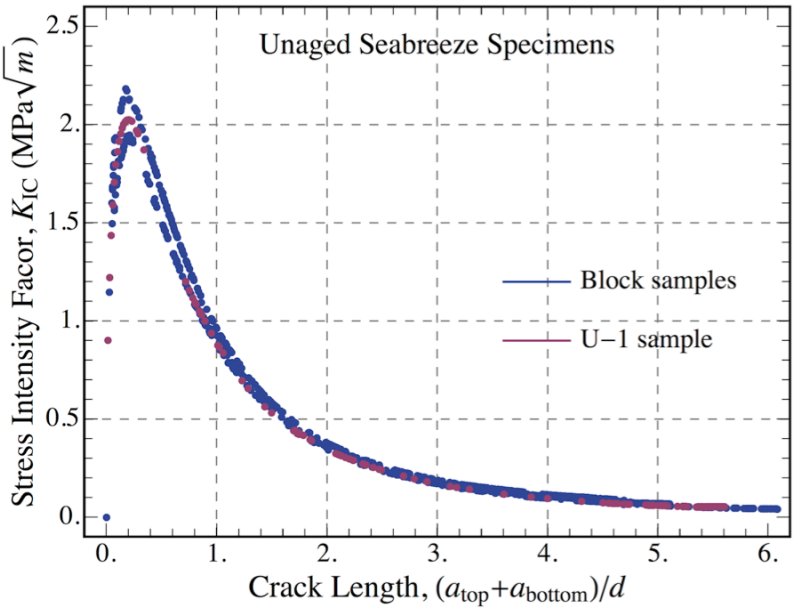

Figure 43. Summary plot for the critical stress intensity factor for un-aged seabreeze compression fracture sample with a center hole.

Figure 44 is a summary plot of the aged seabreeze, again very little difference is seen in the 6 tests. The last figure is a plot comparing the un-aged and aged material (Fig. 45). This plot shows that within scatter there is no effect of aging on the stress intensity factor (fracture toughness) for this material to the assumed artificial age.

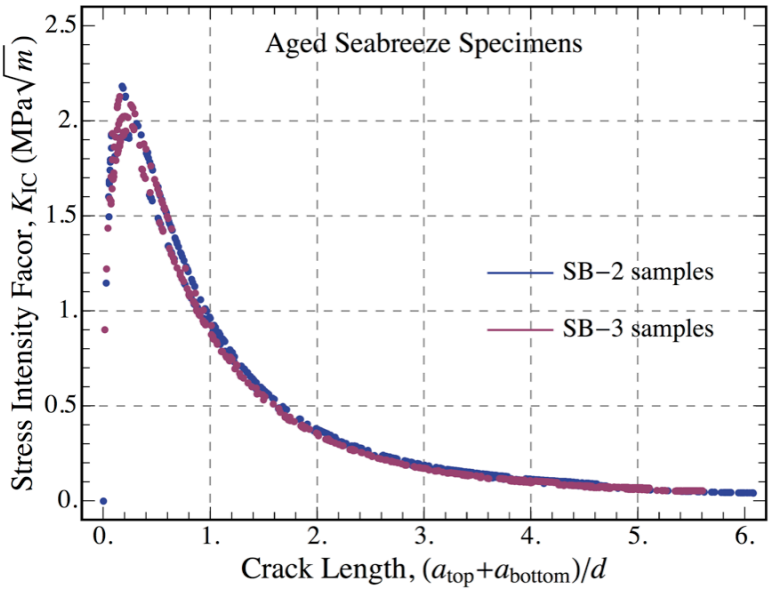

Figure 44. Summary plot for the critical stress intensity factor for aged seabreeze compression fracture sample with a center hole. This plot shows results for both un-pedigreed and pedigreed materials.

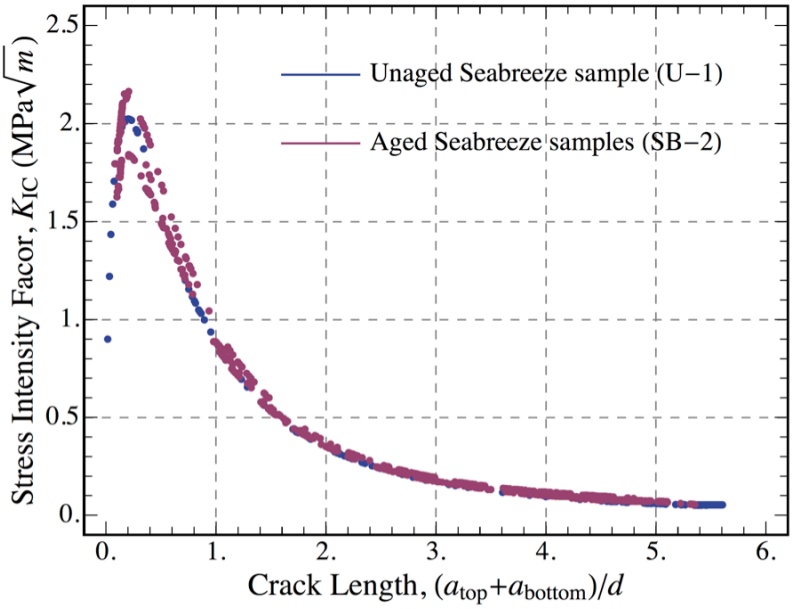

Figure 45. Comparison plot for the critical stress intensity factor for pedigreed seabreeze in both un-aged and the aged condition for the compression fracture sample with a center hole.

Summary

The process by which the final experimental sample geometry is described in this report. Through investigation of the fracture process in both DAP and seabreeze the development of the final test geometry was achieved. The results show that although changes are minimal it is possible to show that aging does change the fracture toughness of these materials.

Preliminary experimental investigation on the fracture toughness of both DAP and Seabreeze were conducted using the compression of Brazilian disk with a center hole. These test were successful for the DAP material but lead to the conclusion that failure in the seabreeze was to rapid for accurate readings of the fracture toughness using this test geometry.

The digital image correlation (DIC) was used to capture the deformation field on sample surfaces. A scheme for quantifying the extent of damage and cracking was also employed to determine the moment of crack initiation and the history of crack growth. This information was used to calculate the fracture toughness once the images were fully characterized. The DAP samples showed sizable and easily measureable crack growth rates that allowed for an easy calculation for the fracture toughness using both the Brazil test and the compression fracture test. The seabreeze material showed very short crack growth prior to the final brittle failure and prohibited the application of conventional fracture mechanics analysis for extracting fracture toughness information. A comparison of the DAP material to the seabreeze material showed significantly less local and overall deformation in the seabreeze at the moment of failure. These results led to the development of a new test configuration, a compression-fracture sample with a center hole, that demonstrated that the crack growth was stable and would allow us to measure the crack growth as a function of load. This information could then be used to calculate the fracture toughness of both DAP and Seabreeze.

The solution for the stress intensity factor is a semi-empiricial in nature and has many assumptions and constraints and therefore may not be ideal for our sample geometries. However, we are exploring alternative ways to extract the fracture toughness information form the recorded experimental results. One of the benefits is using the DIC technique is that it allows for re-evaluation of the test at any time in the future since the entire test is recorded for evaluation. Some additional tests may be needed to determine elastic constants like Young's Modulus and Poisson's ratio, but these tests are easy to conduct and well understood. We are currently looking into a finite element based solution for the fracture toughness measurement that could lead to a engineering value for this property.

references

[1] Sutton, M.A., McNeill, S.R., Helm, J.D., and Chao, Y.J. (2000) Advances in Two-Dimensional and Three-Dimensional Computer Vision, Topics Appl. Phys. **77**, 323–372

[2] Huang, et al., Acta Mat 1996

[3] Liu, et al., Int J Fract 1997).

[4] Sammis and Ashby, "The Failure of Brittle Porous Solids Under Compressive Stress States" *Acta Metall*., 34, 1 (1986) 511-526

[5] Nemat-Nasser